

# 1 Wastewater SARS-CoV-2 Concentration and Loading Variability from Grab and 24- 2 Hour Composite Samples

3

4 Kyle Curtis, David Keeling, Kathleen Yetka, Allison Larson, Raul Gonzalez\*

5 Hampton Roads Sanitation District, 1434 Air Rail Avenue, Virginia Beach, VA 23455

6

7 \*Corresponding author email: [rgonzalez@hrsdc.com](mailto:rgonzalez@hrsdc.com)

8

9

## 10 Abstract

11 The ongoing COVID-19 pandemic caused by severe acute respiratory syndrome coronavirus 2 (SARS-  
12 CoV-2) requires a significant, coordinated public health response. Assessing case density and spread of  
13 infection is critical and relies largely on clinical testing data. However, clinical testing suffers from  
14 known limitations, including test availability and a bias towards enumerating only symptomatic  
15 individuals. Wastewater-based epidemiology (WBE) has gained widespread support as a potential  
16 complement to clinical testing for assessing COVID-19 infections at the community scale. The efficacy of  
17 WBE hinges on the ability to accurately characterize SARS-CoV-2 concentrations in wastewater. To date,  
18 a variety of sampling schemes have been used without consensus around the appropriateness of grab or  
19 composite sampling. Here we address a key WBE knowledge gap by examining the variability of SARS-  
20 CoV-2 concentrations in wastewater grab samples collected every 2 hours for 72 hours compared with

21 corresponding 24-hour flow-weighted composite samples. Results show relatively low variability (mean  
22 for all assays = 741 copies 100 mL<sup>-1</sup>, standard deviation = 508 copies 100 mL<sup>-1</sup>) for grab sample  
23 concentrations, and good agreement between most grab samples and their respective composite (mean  
24 deviation from composite = 159 copies 100 mL<sup>-1</sup>). When SARS-CoV-2 concentrations are used to  
25 calculate viral load, the discrepancy between grabs (log<sub>10</sub> difference = 12.0) or a grab and its associated  
26 composite (log<sub>10</sub> difference = 11.8) are amplified. A similar effect is seen when estimating carrier  
27 prevalence in a catchment population with median estimates based on grabs ranging 62-1853 carriers.  
28 Findings suggest that grab samples may be sufficient to characterize SARS-CoV-2 concentrations, but  
29 additional calculations using these data may be sensitive to grab sample variability and warrant the use  
30 of flow-weighted composite sampling. These data inform future WBE work by helping determine the  
31 most appropriate sampling scheme and facilitate sharing of datasets between studies via consistent  
32 methodology.

33

34

35

## 36 Introduction

37 The outbreak of the novel severe acute respiratory syndrome coronavirus 2 (SARS-CoV-2) in late 2019  
38 escalated to a global pandemic. To date (7-1-2020) there are over 10.5 million confirmed cases and  
39 500,000 deaths world-wide attributed to COVID-19, the disease caused by SARS-CoV-2.<sup>1</sup> Understanding  
40 the extent and density of infection is critical in effectively responding to this pandemic. However, due to  
41 limited diagnostic testing<sup>2,3</sup> and inconsistent reporting of results<sup>4</sup>, generating reliable COVID-19

42 prevalence estimates in a community remains challenging. This is compounded by asymptomatic  
43 disease transmission, the rate of which is still unclear<sup>5</sup>.

44 Wastewater-based epidemiology (WBE) represents a promising complement to clinical testing as a  
45 means of assessing COVID-19 trends and prevalence within a community. WBE has been used to  
46 investigate occurrence and trends for a variety of chemical (pharmaceuticals<sup>6</sup>, illicit drugs<sup>7</sup>) and  
47 biological (pathogens<sup>8</sup>, antibiotic resistance genes<sup>9</sup>) constituents at the community-scale by measuring  
48 biomarkers in wastewater. Unlike clinical testing data, which is susceptible to biases such as test  
49 availability and the inability to detect asymptomatic individuals, WBE yields a community-scale viral load  
50 estimate for a wastewater treatment plant catchment population. Considering these benefits, there has  
51 been much support for WBE as a complementary strategy to clinical testing in response to the SARS-  
52 CoV-2 pandemic.<sup>9,10, 11</sup>

53 The use of WBE in a variety of geographically and demographically disparate areas creates the  
54 opportunity to coordinate efforts, assimilate data, and assess SARS-CoV-2 trends on a larger scale than  
55 any single WBE study could alone. For this broad, integrated approach to succeed many knowledge  
56 gaps must first be addressed for appropriate data comparisons. Such areas include sample collection,  
57 preservation, concentration, and quantification in a complex and challenging wastewater  
58 matrix.<sup>9,12,13,14,15</sup> A fundamental study design knowledge gap considers how to collect a sample that is  
59 appropriately representative of SARS-CoV-2 concentrations in wastewater. Given that influent flows at  
60 wastewater facilities fluctuate continually it is important to understand if these variations in flow  
61 correspond to significant virus concentration variation. Specifically, do grab samples sufficiently  
62 characterize wastewater SARS-CoV-2 concentrations, or are flow-weighted composites necessary?

63 We address this knowledge gap via a comparison of grab and 24-hr flow-weighted composite samples  
64 over a 3-day intensive time series. The goal was to characterize SARS-CoV-2 variability in grab samples

65 collected every 2hrs for 72 hours and compare this variability with 3 flow-weighted composites collected  
66 over the same time frame. Specific objectives are; 1) to examine the variability of reverse transcription  
67 droplet digital PCR (RT-ddPCR) quantified SARS-CoV-2 concentrations, 2) compare instantaneous loading  
68 calculations from grab sample concentrations with loading calculations using respective 24-hr flow-  
69 weighted composite concentrations, and 3) compare instantaneous carrier prevalence estimates from  
70 grab sample concentrations with carrier prevalence estimates using respective 24-hr flow-weighted  
71 composite concentrations.

72 This work will aid future WBE studies in determining the most appropriate sampling scheme. Increasing  
73 the chance of accurately characterizing SARS-CoV-2 concentrations in wastewater allows WBE work to  
74 provide the best available data for use in subsequent calculations, such as estimates of carrier  
75 prevalence or epidemiological models.

76

## 77 Methods

### 78 *Wastewater Treatment Facility*

79 Army Base Treatment Plant (ABTP) is in Norfolk, VA, and is operated by Hampton Roads Sanitation  
80 District (HRSD). It services an area of approximately 21 square miles, which is dominated by residential  
81 development, a port, and a large military base. The treatment plant serves a population of  
82 approximately 78,322, however this figure can fluctuate considerably due to the arrival and departure of  
83 military vessels and cargo ships. A further consideration is that the population of a catchment can vary  
84 based on redirection of flow throughout the collection system, a practice that is common for  
85 wastewater utilities.

86 For ABTP, pretreatment involves coarse screening via bar screens. Residual suspended solids, fats, oils,  
87 and grease are removed during a primary settling step. Secondary treatment consists of a 5-stage  
88 Bardenpho system and secondary settling. Secondary clarifier effluent is disinfected with sodium  
89 hypochlorite and dechlorinated via sodium bisulfite prior to discharge. ABTP has a design flow of 18  
90 MGD with a peak capacity of 36 MGD, and average daily flows ranging 10-11 MGD. Over the three-day  
91 study period, the average daily flow was 12.46 MGD.

#### 92 *Study Design*

93 Samples were aseptically collected over a 72-hour period (5/1/2020 10:00 EST– 5/4/2020 10:00 EST)  
94 from the ABTP Raw Water Influent (RWI) sample point prior to pretreatment. Uniform 1L grab samples  
95 were collected every two hours using an ISCO Avalanche portable refrigerated sampler (Teledyne ISCO,  
96 Lincoln, NE) which kept the samples at approximately 4°C. For each 24-hour period, a flow-weighted  
97 composite sample was collected concurrently with the sequentially collected grabs using an ISCO 3710  
98 Portable sampler (Teledyne ISCO). The composite sampler was paced to take a 150mL aliquot every  
99 230,000 gallons, with all aliquots collected in a sterile 15L carboy in a sampler base filled with ice that  
100 was replenished daily. Final Effluent (FNE) samples were collected aseptically after the 30-minute  
101 chlorine contact point between mid-morning and mid-day of each collection. Each set of 24-hour  
102 composite samples were transported on ice from the sampling site to the HRSD Central Environmental  
103 Laboratory (within 4 hours) where samples were processed upon arrival.

#### 104 *Sample Processing*

105 Electronegative filtration, following the method in Worley-Morse et al<sup>14</sup>, was used to concentrate SARS-  
106 CoV-2 from 50 mL of raw wastewater and 200 mL of treated final effluent. Filters were stored in a -80°C  
107 freezer immediately after concentration until RNA extraction using the NucliSENS easyMag (bioMerieux  
108 Inc., Durham, NC, USA) modified protocol described in Worley-Morse et al. RT-ddPCR was used to

109 enumerate SARS-CoV-2 N1, N2, and N3 assays<sup>16</sup> and the hepatitis G inhibition control on a Bio-Rad

110 QX200 (Bio-Rad, Hercules, CA, USA) using the protocol in Gonzalez et al.<sup>17</sup>

111 *Estimating SARS-CoV-2 Infections in the Sewage Collection System*

112 A promising extension of WBE is calculating prevalence estimates to better gauge the number of truly

113 infected individuals (both symptomatic and asymptomatic). This approach has been used in several

114 recent SARS-CoV-2 publications.<sup>11,18,19</sup> The number of SARS-CoV-2 infected carriers for the ABTP service

115 area were estimated using two values—viral load per person and total viral load to a treatment facility.

116 For the purpose of viral load and carrier prevalence estimates, only the N2 assay was used. Equation 1

117 was used to calculate the viral load per person (the total amount of virus shed by an infected person via

118 feces). The 90<sup>th</sup> percentile concentration of SARS-CoV-2 in stool reported from Wölfel et al.<sup>20</sup> was used

119 was variable A in equation 1. A triangular distribution (minimum= 51, likeliest= 128, maximum= 796) for

120 the fecal mass per person per day, variable B, was fitted from Rose et al.<sup>21</sup> This distribution was sampled

121 during each of 10,000 Monte Carlo simulations conducted using Oracle Crystal Ball (Oracle, Berkshire,

122 UK).

123 Equation 1.

124 
$$Load_{indiv} = C_{indiv} \times m$$

125 where;

126  $Load_{indiv}$  = Viral load per person (copies day<sup>-1</sup>)

127  $C_{indiv}$  = concentration of SARS-CoV-2 virus in feces (copies g<sup>-1</sup>)

128  $m$  = typical mass of stool produced per person per day (g day<sup>-1</sup>)

129 Total viral load to each WWTP during each sampling event was calculated using equation 2. In order to  
130 quantify any potential carriers in the population the N2 assay concentration for each sample was used  
131 as the  $C_{WWTP}$  value in Equation 2.

132 Equation 2.

133

$$Load_{WWTP} = C_{WWTP} \times Q \times f$$

134 where;

135  $Load_{WWTP}$  = Viral load to WWTP (copies day<sup>-1</sup>)

136  $C_{WWTP}$  = concentration of SARS-CoV-2 in wastewater samples (copies 100 mL<sup>-1</sup>)

137  $Q$  = Plant flow (MGD, million gal day<sup>-1</sup>)

138  $f$  = Conversion factor between 100 mL and MG

139

140 Prevalence estimates were calculated using equation 3, which incorporated results from equations 1  
141 and 2 for each sampling event. There is a possibility of asymptomatic carriers, those within higher age  
142 groups, or individuals with co-morbidities shedding a higher range of viruses per stool event. However,  
143 this cannot be accounted for in the population within the WWTP service area since shedding rates for  
144 specific populations are unknown. Subsequently, attempting to adjust the population or the shedding  
145 rates for these differences would require the use of data from other viruses, and would potentially  
146 impart confounding factors in the estimate.

147 Equation 3.

148

$$I = \frac{Load_{WWTP}}{Load_{indiv}}$$

149 where;

150  $I$  = Estimated proportion of WWTP service area infected

151

## 152 *Data Analysis and Visualization*

153 Data analysis and visualization was conducted using R Statistical Computing Software version 3.6.3.<sup>22</sup>

154 The dplyr<sup>23</sup> and tidyr<sup>24</sup> packages were primarily used for data manipulation and the ggplot2 package<sup>25</sup>

155 was used for all plotting. The code used to create each figure can be found at

156 [https://github.com/mkc9953/WW\\_EPI\\_grab\\_composite\\_study](https://github.com/mkc9953/WW_EPI_grab_composite_study).

157

## 158 Results and Discussion

159 Three large wastewater facilities collect and treat portions of the city of Norfolk's wastewater. The ABTP

160 currently receives wastewater from approximately 36% of the city's population. During the study period

161 there was 211, 211, and 239 clinically confirmed COVID-19 cases in the entire city (for days 1, 2, and 3,

162 respectively). Gonzalez et al.<sup>17</sup> has been monitoring this facility, amongst others, weekly since March 9<sup>th</sup>,

163 2020. Detections of SARS-CoV-2 began on April 6, 2020—4 weeks prior to this study.

## 164 *Influent Flow and Rainfall*

165 Hourly wastewater influent flow during the study period ranged from 7.16 to 16.28 million gallons per

166 day (MGD), with a mean flow of 12.3 MGD and standard deviation of 2.73 MGD. A description of flow

167 characteristics by sample day can be found in Table 1. Two days prior to the first sampling event there

168 was a storm generating approximately 1.0 inches of rainfall. A brief increase in flow was observed, likely

169 due to stormwater infiltrating the sewer collection system. Influent flow at the treatment facility



170 returned to typical dry weather values in approximately 6hrs and remained at levels typical of dry  
171 weather throughout the study. No rainfall occurred in the vicinity of the treatment facility during the  
172 study period. The treatment facility serves several low-lying areas that are subject to inundation during  
173 moderate high tide events, causing saltwater intrusion into sewer collection system. Treatment plant  
174 influent conductivity, used as an indicator of seawater, begins to increase significantly following tidal  
175 levels greater than 3.5' Mean Lower Low Water (MLLW). High tides during the period sampled were 3.4'  
176 MLLW or less based on the Sewell's Point Tide Gage operated by NOAA.

### 177 *SARS-CoV-2 Concentration and Variability*

178 All three assays used for this study (N1, N2, N3) yielded positive results for every raw wastewater  
179 influent sample. All three final effluent samples were below the limit of detection (LOD = 58 copies/100  
180 mL). For composite samples, concentrations of all assays ranged from 580 – 1380 copies 100 mL<sup>-1</sup>, with  
181 a mean of 900 and standard deviation of 215 copies 100 mL<sup>-1</sup>, showing good agreement across the three  
182 days (Figure 1). Similarly, composite samples showed relatively low variability within (largest range =  
183 490 copies 100 mL<sup>-1</sup>) and between assays (largest range = 580 copies 100 mL<sup>-1</sup>) for a given day (Table 2).  
184 Grab sample concentration variability was also low, ranging from 25 to 1100 copies 100 mL<sup>-1</sup> for all  
185 samples collected (Table 3) with a coefficient of variation (CV) of 68.5%. Grab sample concentrations  
186 showed good agreement across assays as means, minima, and maxima were each in the same  
187 respective order of magnitude (Table 3). Examining the association between each possible pair of assays  
188 showed a positive monotonic relationship for all combinations, with Pearson coefficients ranging 0.72-  
189 0.90 (Figure 2). Comparing results by day for all assays showed similarly low variability with the greatest  
190 difference in any two daily mean concentrations of 114.8 copies 100 mL<sup>-1</sup> (Table 3).  
191 Grab sample concentrations showed good agreement with corresponding composite concentrations  
192 (Figure 1), with a mean deviation of 159 copies 100 mL<sup>-1</sup> between a grab sample and its associated

193 composite. Over half of the total number of grab samples (59/108) had concentrations which were  
194 within 50% of their respective composite. Interestingly, the discrepancy between grab and composite  
195 concentrations, regardless of magnitude, often (75/108) showed grabs at lower concentration than the  
196 corresponding composite (Figure 1). These drops in virus concentration were not concurrent with times  
197 of lowest influent flow but seemed to lag by approximately 4-6hrs (Figure 1). This pattern may be  
198 influenced by the number and density of COVID-19 infections in the region. In a case with few infected  
199 individuals the viral signal would be sporadic in the daily flow. Conversely, if a catchment area were  
200 highly impacted by infections, the virus signal in wastewater would be less variable and minimally  
201 influenced by changes in flow. The ABTP catchment could have a high enough infection density to  
202 consistently detect a wastewater signal, but not so ubiquitous that the signal is entirely unimpacted by  
203 diurnal cycles in flow. Considering this, grab samples should be collected at times that avoid early  
204 morning flow minima and the subsequent 4-6hrs dips in viral concentration, in order to avoid  
205 underestimating viral load to the treatment facility.

206

### 207 *Viral Load and Carrier Prevalence*

208 Wastewater N2 SARS-CoV-2 concentrations were used to calculate viral load for grab and composite  
209 samples (Figure 3). Viral loads calculated using composite sample values showed low variability between  
210 days, ranging from  $4.2 \times 10^{11}$  –  $6.3 \times 10^{11}$ . Variability in instantaneous load derived using grab sample  
211 concentrations was greater, ranging from  $3.7 \times 10^{10}$  –  $1.11 \times 10^{12}$ , with a mean of  $4.1 \times 10^{11}$  and standard  
212 deviation of  $2.8 \times 10^{11}$ . While the variability in grab sample concentration (CV=68.5%) and viral load  
213 calculated from grab sample concentration (CV=69.3%) are expectedly similar, the magnitude of any  
214 given deviation in viral load is increased due to the way load is derived (Equation 2). For example, the  
215 greatest difference in concentration between a grab and composite sample, within a common assay,

216 was 1340 copies 100 mL<sup>-1</sup>. When viral load is calculated using this same grab and composite the  
217 difference between the two types of sample is 2.8\*10<sup>11</sup> copies 100 mL<sup>-1</sup>. For all load calculations using  
218 grab sample values, the mean deviation from the corresponding composite value was 8.4 \*10<sup>10</sup>, or  
219 14.9%. Data presented here demonstrate the potentially large disparity in viral load values calculated  
220 using SARS-CoV-2 concentrations given a difference in only 2hrs between grab sample collection times.  
221 For this study grab samples more often had lower concentrations than the corresponding composite,  
222 thus there is a higher likelihood of underestimating concentrations when collecting grabs. Viral  
223 concentration data which are biased low will affect downstream calculations made using these data,  
224 such as estimates of viral load and carrier prevalence in the catchment population. If these metrics are  
225 used to inform a public health response it is critical that they do not systematically underestimate the  
226 extent of COVID-19 infections in the community.

227

228 SAR-CoV-2 concentrations in wastewater can also be used to estimate the prevalence of carriers in a  
229 catchment population (Equation 3). Currently there is considerable uncertainty around the viral  
230 shedding rate in feces of people infected with COVID-19. A widely reference paper by Wölfel et al.  
231 examining nine clinical cases found concentrations of SARS-CoV-2 viral RNA in stool ranging from below  
232 the limit of detection to 7.1\*10<sup>8</sup> copies 100 mL<sup>-1</sup>.<sup>20</sup> Furthermore, a sensitivity analysis of previous  
233 carrier prevalence model iterations highlights the high susceptibility to the shedding rate variability,  
234 increasing the error associated with resulting estimates. However, as viral shedding rate is more fully  
235 described, carrier estimates could become increasingly important, given the potential public health  
236 value in generating a reliable estimate of infected people in a catchment. Results of this study highlight  
237 the importance of collecting a sample that is representative of SARS-CoV-2 concentrations in  
238 wastewater, as subsequent viral load and carrier estimates are based on this value. As with viral

239 concentration and viral load data, variability in was low in carrier estimates for composite samples with  
240 median values of 703, 1057, 709 copies 100 mL<sup>-1</sup> (Figure 3). When including the 10<sup>th</sup> and 90<sup>th</sup> percentile  
241 results, estimates ranged from 365 to 2474 carriers in the catchment for composite samples. Carrier  
242 estimates based on grab samples were more variable, with an overall range of 32 to 4336 carriers, and  
243 median estimates ranging from 62-1853 carriers. The median carrier estimate from 24 of 36 grab  
244 samples fell within the 10<sup>th</sup>-90<sup>th</sup> percentile range for the corresponding composite. Of the 12 grabs for  
245 which the median carrier estimate was outside of the composite estimate 10<sup>th</sup> – 90<sup>th</sup> range, 11 were  
246 below the composite estimate range and 4 showed no overlap between the grab and composite (10 –  
247 90<sup>th</sup> percentile) ranges. Because these calculations are based on viral concentration it was expected that  
248 estimates from grabs would more often be lower than estimates made using composite concentrations.  
249 For these data, the potential underestimation of median carrier prevalence due to collecting a grab  
250 sample rather than a composite could be as large as 995 people, based on the minimum median carrier  
251 estimate (62) and corresponding composite estimate (1057) (Figure 3). That discrepancy in estimated  
252 carriers has practical implications if WBE is used as a component of the public health response to the  
253 SARS-CoV-2 pandemic. Choosing an appropriate sampling scheme can minimize potential bias  
254 introduced into these estimates by accurately characterizing viral concentration. If replication in other  
255 studies shows that grab samples reliably underestimate viral concentration, then either composite  
256 sampling or grab samples targeting the expected peak viral concentration should be employed to reduce  
257 the likelihood of generating data which are biased low.

258

### 259 *Limitations and Future Work*

260 One important consideration for using WBE to examine viral trends during a pandemic is the  
261 heterogenous and dynamic nature of the spread of infections. Epidemiological work has shown that,

262 particularly during the early stages of pathogen spread, rates of infection are not uniform but rather  
263 clustered in localized hotspots often driven by importation of cases<sup>26</sup>, and the disproportionate effects  
264 of “superspreading” events<sup>27</sup>. Interpreting WBE data is also confounded by transient use of the  
265 sewerage system from people who may be infected by do not live in the catchment area, e.g. tourists or  
266 people who commute to a different area for work. Restrictions such as stay-at-home orders and the  
267 subsequent reopening of cities add further complexity to the characteristics of viral spread in a  
268 community. As a result, extrapolation of findings from one catchment to the surrounding region are  
269 not often appropriate. Therefore, data and patterns presented here pertain to this specific catchment  
270 over a 3-day period, and do not easily extend to other areas or timeframes. To address this, we suggest  
271 a surveillance approach to WBE, monitoring multiple catchments on a routine basis<sup>17</sup> to characterize  
272 trends specific to a region over time. As noted, variability in influent concentration change as density of  
273 cases increase or decrease within the catchment. Calculations using influent flow, such as viral load and  
274 carrier prevalence, will also be influenced by diel and seasonal changes in influent flow volume as well  
275 as short term increases due to wet weather. Regular monitoring of facilities reduces some uncertainty  
276 by establishing a context for changes in viral loading. Though estimating carrier prevalence remains  
277 challenging due to uncertainty around viral shedding rates, tracking viral load from a catchment over  
278 time may be sufficient to gain insight into community-level trends.

279

280

281 Acknowledgements

282

283

284

285 References

- 286 1. Dong, E.; Du, H.; Gardner, L. An Interactive Web-Based Dashboard to Track COVID-19 in Real  
287 Time. *Lancet Infect. Dis.* 2020, 3099 (20), 19– 20, DOI: 10.1016/S1473-3099(20)30120-1
- 288 2. Babiker, A.; Myers, C.W.; Hill, C.E.; Guarner, J. SARS-CoV2-2 Testing: Trials and Tribulations. *Am. J. of*  
289 *Clin. Pathol.* 2020, (153) 706-708
- 290 3. Schneider, E.C. Failing the Test- The Tragic Data Gap Undermining the U.S. Pandemic Response. *N.*  
291 *Engl. J. Med.* 2020, DOI: 10.1056/NEJMp2014836
- 292 4. [https://www.richmond.com/special-report/coronavirus/virginia-misses-key-marks-on-virus-testing-](https://www.richmond.com/special-report/coronavirus/virginia-misses-key-marks-on-virus-testing-as-leaders-eye-reopening/article_021e12c6-6d20-5030-9068-4caaeda495f7.html)  
293 [as-leaders-eye-reopening/article\\_021e12c6-6d20-5030-9068-4caaeda495f7.html](https://www.richmond.com/special-report/coronavirus/virginia-misses-key-marks-on-virus-testing-as-leaders-eye-reopening/article_021e12c6-6d20-5030-9068-4caaeda495f7.html)
- 294 5. Kronbichler, A.; Kresse, D.; Yoon, S.; Lee, K.W.; Effenberger, M.; Shin, J.I. Asymptomatic patients as a  
295 source of COVID-19 infections: A systematic review and meta-analysis. *Int. J. Infect. Dis.* 2020, In  
296 Press. DOI: 10.1016/j.ijid.2020.06.052
- 297 6. Choi, P.M.; Tschärke, B.J.; Donner, E.; O'Brien, J.W.; Grant, S.C.; Kaserzon, S.L.; Mackie, R.; O'Malley,  
298 E.; Crosbie, N.D.; Thomas, K.V; Mueller, J.F. Wastewater-based epidemiology biomarkers: past,  
299 present and future. *Trend. Anal. Chem.* 2018, (105) 453-469.
- 300 7. Been, F.; Rossi, L.; Ort, C.; Rudaz, S.; Delémont, O.; Esseiva, P. Population normalization with  
301 ammonium in wastewater-based epidemiology: Application to illicit drug monitoring. *Environ. Sci.*  
302 *Technol.* 2014, 48(14), 8162-8169.
- 303 8. Sims, N.; Kasprzyk-Hordern, B. Future perspectives of wastewater-based epidemiology: Monitoring  
304 infectious disease spread and resistance to the community level. *Environ. Int.* 2020, (139), DOI:  
305 10.1016/j.envint.2020.105689.

- 306 9. Bivens A.; .... Bibby, K. Wastewater-Based Epidemiology: Global Collaborative to Maximize  
307 Contributions in the Fight Against COVID-19. *Environ. Sci. Technol.* 2020, DOI:  
308 10.1021/acs.est.0c02388.
- 309 10. Hata, A.; Honda, R. Potential Sensitivity of Wastewater Monitoring for SARS-CoV-2: Comparison with  
310 Norovirus Cases. *Environ. Sci. Technol.* 2020, DOI: 10.1021/acs.est.0c02271.
- 311 11. Ahmed, W.; ..... Mueller, J.F. First confirmed detection of SARS-CoV-2 in untreated wastewater in  
312 Australia: A proof of concept for the wastewater surveillance of COVID-19 in the community. *Sci.*  
313 *Total Environ.* 2020, (728) 138764.
- 314 12. Mao, K.; Zhang, K.; Du, W.; Ali, W.; Feng, X.; Zhang, H. The potential of wastewater-based  
315 epidemiology as surveillance and early warning of infectious disease outbreaks. *Curr. Opin. Environ.*  
316 *Sci. Health.* 2020, (17), 1-7.
- 317 13. Daughton, C. The international imperative to rapidly and inexpensively monitor community-wide  
318 COVID-19 infection status and trends. *Sci. Total Environ.* 2020, (726) 138149
- 319 14. Worley-Morse, T.; Mann, M.; Khunjar, W.; Olabode, L.; Gonzalez, R. Evaluating the fate of bacterial  
320 indicators, viral indicators, and viruses in wastewater resource recovery facilities. *Water Environ.*  
321 *Res.* 2019, (91) 830-842.
- 322 15. Kitajima, M.; Ahmed, W.; Bibby, K.; Carducci, A.; Gerba, C.P.; Hamilton, K.A.; Harmoto, E.; Rose, J.B.  
323 SARS-CoV-2 in wastewater: State of the knowledge and reasearch needs. *Sci. Total Environ.* 2020,  
324 (739) 139076.
- 325 16. Centers for Disease Control and Prevention (CDC). CDC 2019-Novel Coronavirus (2019-nCoV) Real-  
326 Time RT-PCR Diagnostic Panel. 2020.
- 327 17. Gonzalez, R.; Curtis, K.; Bivins, A.; Bibby, K.; Weir, M.; Yetka, K.; Thompson, H.; Keeling, D.; Mitchell,  
328 J.; Gonzalez, D. COVID-19 Surveillance in Southeastern Virginia Using Wastewater -Based  
329 Epidemiology. *Water. Res.* 2020, Under Review.

- 330 18. Medema, G.; Heijnen, L.; Elsinga, G.; Italiaander, R.; Brouwer, A. Presence of SARS-Coronavirus-2 in  
331 Sewage and Correlation with Reported COVID-19 Prevalence in the Early Stage of the Epidemic in  
332 the Netherlands. *Environ. Sci. Technol. Lett.* 2020, DOI: 10.1021/acs.estlett.0c00357
- 333 19. Wu, F.; Xiao, A.; Zhang, J.; Gu, X.; Lee, W.L.; Kauffman, K.; Hanage, W.; Matus, M.; Ghaeli, N.; Endo,  
334 N.; Duvallet, C.; Moniz, K.; Erickson, T.; Chai, P.; Thompson, J.; Alm, E. SARS-CoV-2 titers in  
335 wastewater are higher than expected from clinically confirmed cases. *medRxiv*, 2020. doi:  
336 <https://doi.org/10.1101/2020.04.05.20051540>
- 337 20. Wölfel R.; Corman, V.M.; Guggemos, W.; Seilmaier, M.; Zange, S.; Müller, M.A.; Niemeyer, D.; Jones,  
338 T.C.; Vollmar, P.; Camilla, R.; Hoelscher, M.; Bleicker T.; Brunink, S.; Schneider, J.; Ehmann, R.;  
339 Zwirgmaier, K.; Drosten, C.; Wendtner, C. Virological assessment of hospitalized patients with  
340 COVID-19. *Nature*. 2020, (581) 465-469
- 341 21. Rose, C.; Parker, A.; Jefferson, B.; Cartmell, E. The Characterization of Feces and Urine: A Review of  
342 the Literature to Inform Advanced Treatment Technology. *Crit. Rev. Environ. Sci. Technol.* 2015, (45)  
343 1827-1879.
- 344 22. R Core Team (2017). R: A language and environment for statistical computing. R Foundation for  
345 Statistical Computing, Vienna, Austria. URL <https://www.R-project.org/>.
- 346 23. Wickham, H.; Francois, R.; Henry, L.; Müller, K. dplyr: A grammar of data manipulation. R package  
347 version 0.8.5. 2015. <https://CRAN.R-project.org/package=dplyr>
- 348 24. Wickham, H.; Henry, L. tidyr: Easily Tidy Data with 'spread()' and 'gather()' Functions. R package  
349 version 1.0.2. 2018 <https://CRAN.R-project.org/package=tidyr>
- 350 25. Wickham, H. ggplot2: elegant graphics for data analysis. Springer-Verlag New York. 2016, ISBN 978-  
351 3-319-24277-4, <https://ggplot2.tidyverse.org>.



- 352 26. Bajardi, P.; Poletto, C.; Ramasco, J.J.; Tizzoni, M.; Colizza, V.; Vespignani, A. Human Mobility  
353 Networks, Travel Restrictions, and the Global Spread of 2009 H1N1 Pandemic. PLoS One. 2011b,  
354 6(1).
- 355 27. Lipsitch, M.; Cohen, T.; Cooper, B.; Robins, J.M.; Ma, S.; James, J.; Gopalakrishna, G.; Chew S.K.; Tan,  
356 C.C.; Samore, M.H., Fisman, D.; Murray, M. Transmission Dynamics and Control of Sever Acute  
357 Respiratory Disease. Science. 2003, (300) 1966-1970.

358

359

360

361

362

363

364

365

366

367

368

369

370

371

372 Tables

373 1. Influent Flow for Study Period

Influent Flow For Study Period					
	Min	Max	Mean	Standard Deviation	Hour of Peak flow
Day 1	8.18	15.64	12.47	2.60	2000
Day 2	7.86	15.37	12.11	2.79	1200
Day 3	7.16	16.28	12.31	3.02	1200

374

375

376

377 2. SARS-CoV-2 Concentrations in Composite Samples

Composite SARS-CoV-2 Concentration				
Date	Composite	N1	N2	N3
5/2/2020	1	860	890	890
5/3/2020	2	800	1380	1010
5/4/2020	3	580	910	780

378

379

380

381

382

383 3.

Grab Sample SARS-CoV-2 Concentration (copies 100 mL <sup>-1</sup> )				
By Assay				
	N1	N2	N3	Overall
Min	50	90	140	50
Max	2200	2000	2100	1100
Mean	608	848	768	741
St. Dev	501	500	506	508
By Day				
	Day 1	Day 2	Day 3	Overall
Min	220	50	110	50
Max	2200	2100	1800	1100
Mean	759	790	675	726
St. Dev	456	571	497	502

384

385

386

387

388

389

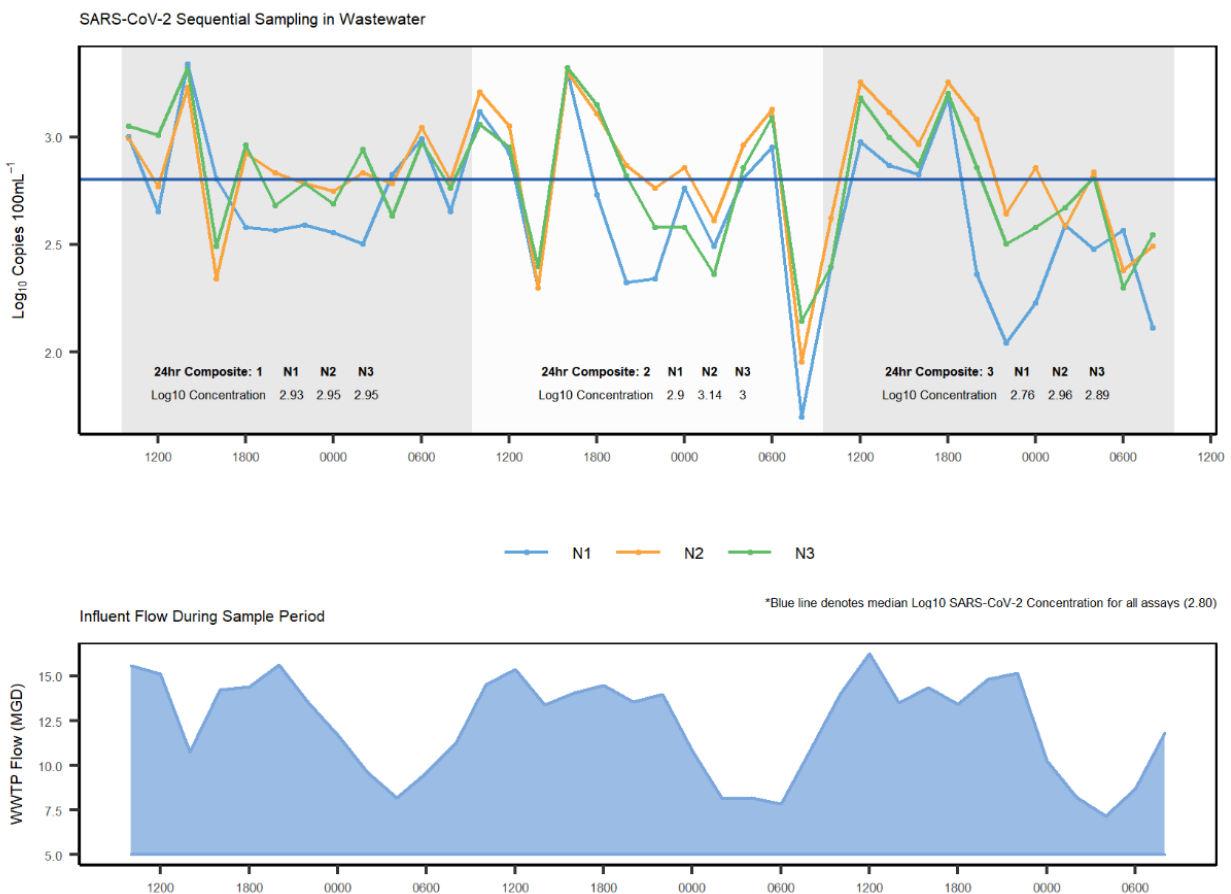
390

391 Figures

392

393 Figure 1.

394 Wastewater  $\log_{10}$  SARS-CoV-2 concentrations (copies  $100\text{ mL}^{-1}$ ). Grab sample concentrations  
395 are denoted by dots with each color representing an assay (N1, N2, N3). Shaded areas denote  
396 the timeframe for three discrete 24hr flow-weighted composites. Concentrations for each  
397 composite sample are noted. Influent flow is plotted in the lower panel.



398

399

400 Figure 2.

401

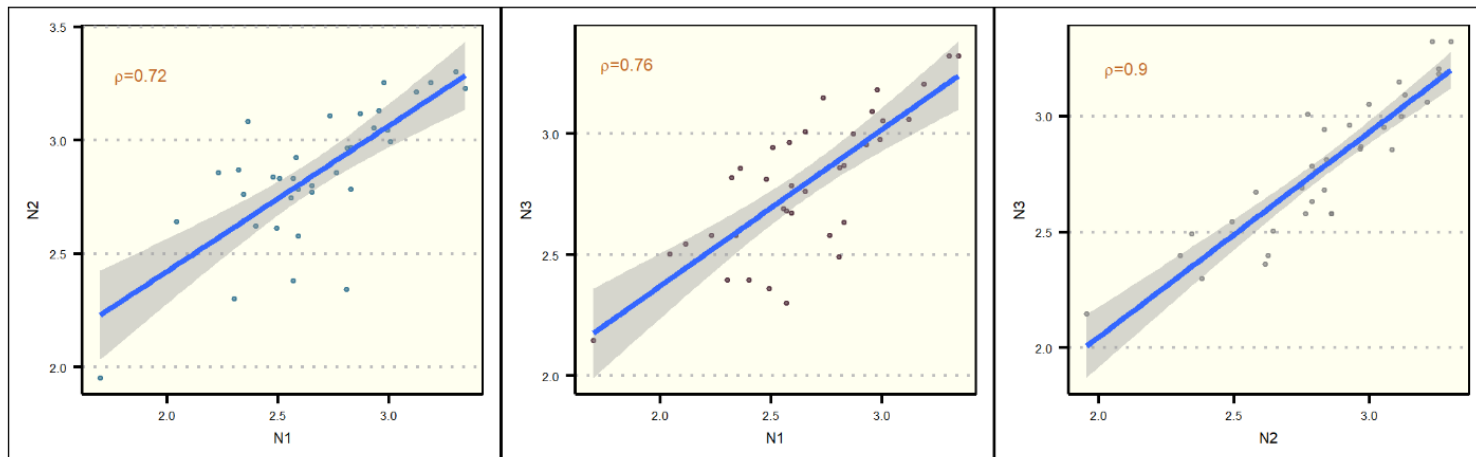
402 Associations between SARS-CoV-2 assays (N1, N2, N3). X and Y axes show  $\log_{10}$  concentrations for each

403 assay. Lines represent linear association between assays, shaded areas denote standard error for

404 regression. Spearman correlation coefficients are listed in orange on each plot.

405

SARS-CoV-2 Assay Comparison



\*Time series of Log10 Concentrations from the same WWTP

406

407

408

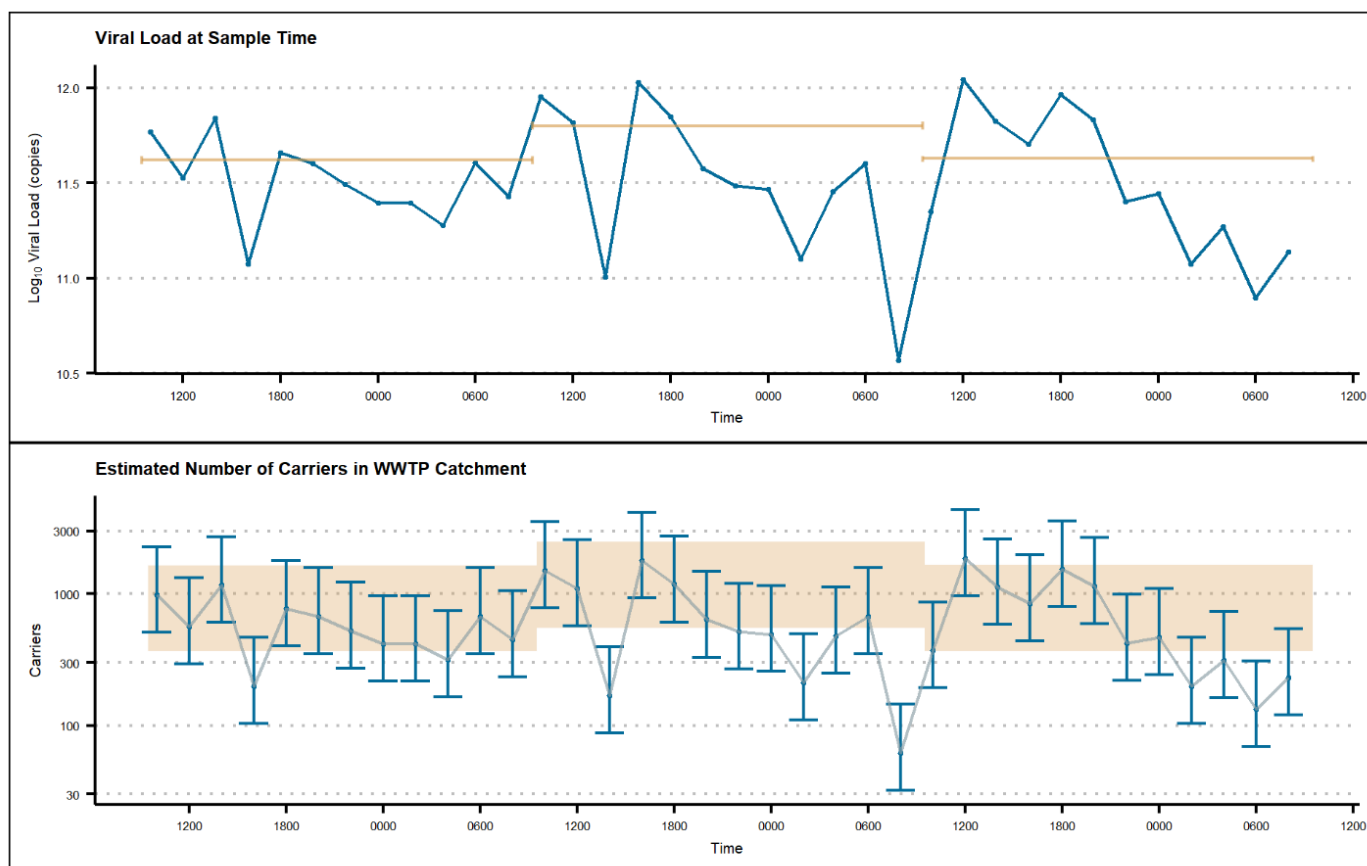
409

410

411

412 Figure 3.

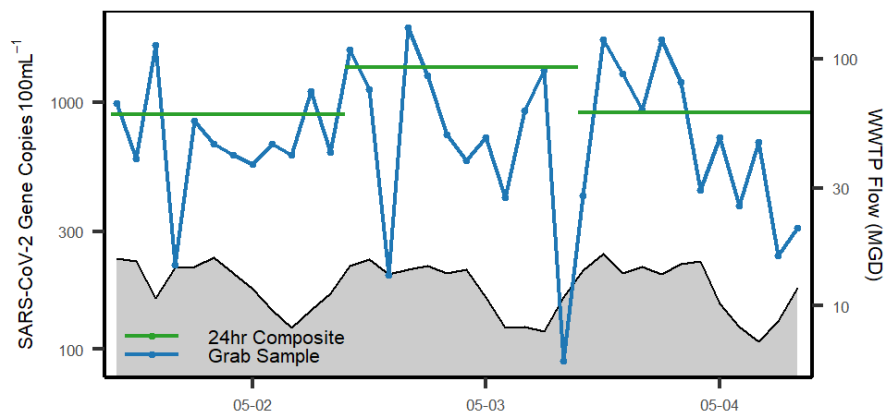
413 Wastewater SARS-CoV-2 load and carrier prevalence estimates for the 72-hour study. For the upper  
414 panel, load ( $\log_{10}$  copies) calculated using grab sample concentrations are denoted by blue dots, while  
415 load ( $\log_{10}$  copies) from 24-hr composite concentrations are denoted by horizontal orange lines. In the  
416 lower panel, prevalence of SARS-CoV-2 infected carriers is estimated using Monte Carlo simulation.  
417 Estimates derived using grab sample concentrations are denoted by blue dots (median number of  
418 carriers) with error bars indicating the 10<sup>th</sup> and 90<sup>th</sup> percentile range in estimates. Shaded areas indicate  
419 the 10<sup>th</sup> to 90<sup>th</sup> percentile range of carrier estimates calculated using 24hr composite samples.



420

421

422 Graphical Abstract – For Table of Contents Only



423